Electronic structure of the quasi-two-dimensional spin-gap system $SrCu_2(BO_3)_2$: Experiment and theory

G. Radtke,[1,*] A. Saúl,[2] H. A. Dabkowska,[3] B. D. Gaulin,[3] and G. A. Botton[4]
[1]*Laboratoire TECSEN, UMR 6122 CNRS, Faculté des Sciences de Saint-Jérôme, Case 262, Université Paul Cézanne-Aix Marseille III, 13397 Marseille Cedex 20, France*
[2]*Centre de Recherche en Matière Condensée et Nanosciences CNRS, Campus de Luminy, Case 913, 13288 Marseille Cedex 9, France*
[3]*Department of Physics and Astronomy, McMaster University, Hamilton, Ontario, Canada L8S 4C6*
[4]*Brockhouse Institute for Materials Research, McMaster University, Hamilton, Ontario, Canada L8S 4M1*
(Received 16 December 2007; published 26 March 2008)

The electronic structure of the quasi-two-dimensional spin-gap system $SrCu_2(BO_3)_2$ is investigated using a combined experimental and theoretical approach based on electron energy loss spectroscopy (EELS) and first-principles band structure calculations. We show that the local-density approximation (LDA)+U method, guided by the experimental O-K edge recorded in EELS, provides a simultaneous accurate description of both low-energy-scale (magnetic) and high-energy-scale (electronic) properties of this magnetic insulator.

DOI: 10.1103/PhysRevB.77.125130 PACS number(s): 71.27.+a, 79.20.Uv, 75.30.Et

I. INTRODUCTION

In the field of low dimensional spin magnetism, copper oxides provide a large number of interesting model systems. Among them, the layered strontium copper borate $SrCu_2(BO_3)_2$ exhibits a number of unique features such as a spin-gapped behavior, unusual magnetic excitations, or magnetization plateaux.[1] Since the work of Kageyama *et al.*,[2] many experimental[3–6] and theoretical[7–11] studies have been carried out to understand the magnetic properties of this compound, the strong interest for this kind of system being further intensified by the observation of pseudospin gap in high T_c superconductors.

This compound crystallizes in a tetragonal structure[12] where layers of $[CuBO_3]^-$ are stacked along the [001] direction and separated by planes of Sr^{2+} ions (Fig. 1). These layers are themselves constituted by triangular BO_3 and rectangular CuO_4 planar groups connected through common oxygen atoms. The Cu atoms belonging to two adjacent CuO_4 groups sharing an edge form a dimer orthogonally connected with the other dimers through the BO_3 groups [Fig. 2(a)]. With their $3d^9$ electronic configuration, the Cu^{2+} ions hold a localized spin $S=1/2$ located on this two-dimensional network of orthogonal dimers [Fig. 2(b)]. Therefore, it has been suggested that the magnetic properties of this compound can be described through a two-dimensional Heisenberg Hamiltonian,[7]

$$H = J\sum_{nn} \mathbf{S}_i \cdot \mathbf{S}_j + J'\sum_{nnn} \mathbf{S}_i \cdot \mathbf{S}_j, \qquad (1)$$

where J and J' are, respectively, the nearest-neighbor (intradimer) and next-nearest-neighbor (interdimer) exchange integrals. This model, proposed by Miyahara and Ueda in 1999, is equivalent to the Shastry–Sutherland model,[13] developed two decades earlier. In the limit where $J \gg J'$, the system appears as a collection of independent dimers. Inversely, when $J \ll J'$, it is topologically equivalent to a square lattice Heisenberg model with nearest-neighbor interactions. Shastry and Sutherland have shown the remarkable property that the Hamiltonian (1) admits the direct product of dimer singlet states as an exact eigenstate. It has been further shown that this $S=0$ wave function is the ground state for a J/J' ratio below a critical value close to 0.7.[7,9,10] A combined analysis of the experimental low temperature magnetic susceptibility and the spin gap Δ_s allowed the determination of these parameters in $SrCu_2(BO_3)_2$: $J=85$ K and $J'=54$ K, giving the ratio $J/J'=0.635$. However, a better fit of the high temperature ($T > \Delta_s$) magnetic susceptibility is only obtained when the effect of a third coupling constant J'' between dimers of adjacent layers is also taken into account,[14] giving $J''=8$ K.

These exchange integrals play a crucial role in determining the magnetic behavior of $SrCu_2(BO_3)_2$ and are intimately related to the underlaying electronic structure of this com-

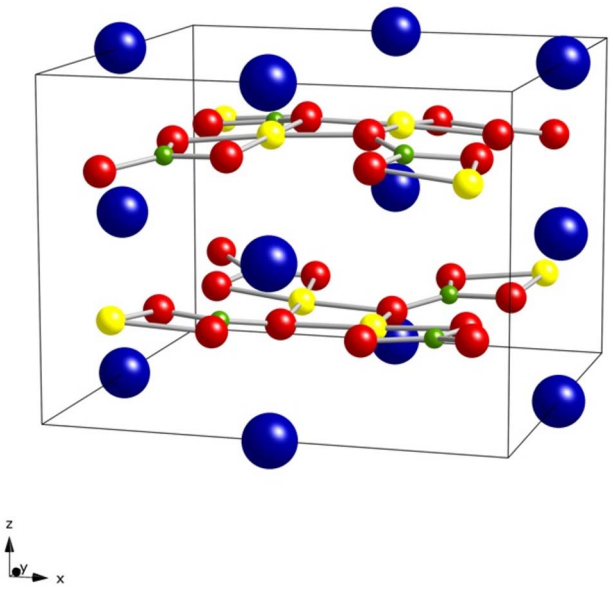

FIG. 1. (Color online) The tetragonal unit cell of $SrCu_2(BO_3)_2$: Sr atoms are in blue, O atoms in red, B atoms in green, and Cu atoms in yellow. The stacking of the $[CuBO_3]^-$ layers along the [001] direction of the crystal separated by Sr^{2+} atoms is clearly visible.

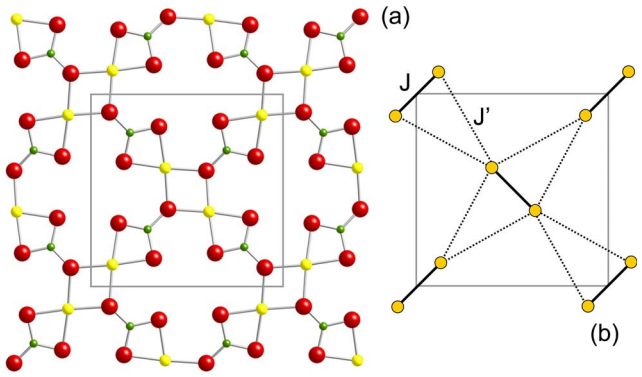

FIG. 2. (Color online) Portion of a $[CuBO_3]^-$ layer in $SrCu_2(BO_3)_2$: (a) The atomic structure: small, green atoms are B atoms, small, yellow atoms are Cu atoms, and large, red atoms are O atoms. (b) Lattice structure of Cu^{2+} spins: solid lines represent the nearest-neighbor interaction J and the dashed lines represent the next-nearest-neighbor interaction J'. The two-dimensional projection of the tetragonal unit cell is also represented.

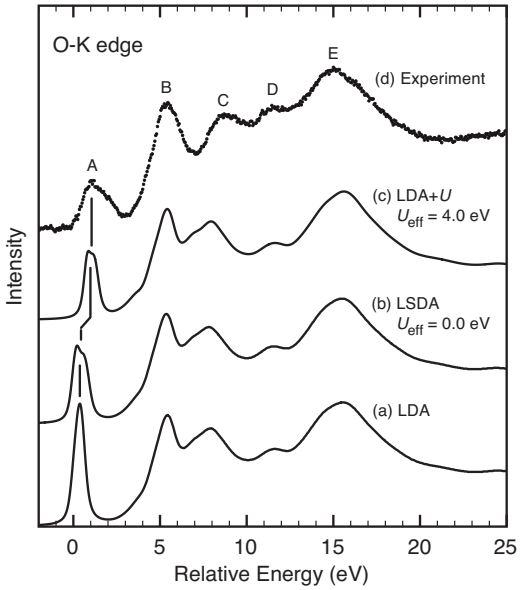

FIG. 3. Comparison between experimental and theoretical *O-K* edge in $SrCu_2(BO_3)_2$: (a) LDA, (b) LSDA (U_{eff}=0.0 eV), (c) LDA+U ($U_{eff}=U-J^H$=4.0 eV), and (d) experiment.

pound. A detailed study of this electronic structure is thus of great interest to understand the origin of the magnetic properties of $SrCu_2(BO_3)_2$. However, the complexity of such a system requires an approach combining experimental solid-state spectroscopy and state-of-the-art electronic structure calculations. Electron energy loss spectroscopy indeed provides considerable information on the unoccupied electronic states of solids, but an accurate interpretation of the experimental data can only be achieved with the help of theoretical calculations. Density functional theory within the local spin density approximation (LSDA) is one of the most popular methods available. However, LSDA has been recognized for a long time to give a poor description of strongly correlated systems such as 3*d* or 4*f* electrons. The so-called local-density approximation (LDA)+U method was developed to overcome these difficulties by introducing an explicit orbital-dependent potential accounting for the strong electron-electron interactions arising in these localized *d* or *f* orbitals.[15] In this paper, we report a detailed study of the electronic structure of $SrCu_2(BO_3)_2$ through a combined analysis of the *O-K* near-edge fine structure recorded in electron energy loss spectroscopy (EELS) and LDA+U electronic structure calculations carried out using the WIEN2K code.[16] Similar approaches have been reported in the literature to successfully improve the description of the electronic structure and the properties of NiO.[17–19] In our study of $SrCu_2(BO_3)_2$, we show that the Cu 3*d* Coulomb effective interactions not only play a prominent role in the electronic structure of this compound, leading to the creation of a correlation gap, but also scale the magnitude of the exchange integrals appearing in the Shastry–Sutherland model.

II. ELECTRONIC STRUCTURE

The WIEN2K program is an implementation of the full potential linearized augmented plane-wave method based on density functional theory. Exchange and correlation have been taken into account in the framework of the LSDA using the functional of Perdew and Wang.[20] These calculations were performed using the experimental crystal structure.[12] Muffin-tin radii were set to 2.45 a.u. for Sr, 1.92 a.u. for Cu, and 1.25 a.u. for O and B atoms. The plane-wave cutoff parameter RK_{max} was set to six for all the calculations presented hereafter. For an accurate calculation of the energy loss spectra up to 25 eV above the Fermi level, the basis set was improved after the self-consistent calculation of the electronic density by increasing the energies of the linearized augmented plane waves by 1 Ry, and the high-lying unoccupied states were recalculated in the new basis.

The electronic structure of cuprate compounds near the Fermi level can be described in a simple manner by considering a $[CuO_4]^{6-}$ cluster. In the tight-binding picture, the only strong covalent interaction arising in this structural unit takes place between Cu $d_{x^2-y^2}$ and O p_x, p_y states and leads to the formation of a low-lying $dp\sigma$ bonding and a highly destabilized $dp\sigma^*$ antibonding orbitals. The remaining Cu 3*d* and O 2*p* states are essentially nonbonding and located in between. The $3d^9$ and $2p^6$ electronic configurations of Cu^{2+} and O^{2-}, respectively, fill these electronic states up to the highest $dp\sigma^*$ orbital, which is only half filled. These simple considerations are confirmed by the results obtained in LDA where the Fermi level crosses a well separated narrow peak located on top of an 8 eV wide valence band.

The experimental *O-K* edge is shown in Fig. 3(d). The spectra were recorded on a FEI 200 keV field emission gun transmission electron microscope (TEM) equipped with a monochromator and a high-energy-resolution spectrometer.[21] The energy resolution, measured as the full width at half maximum of the zero loss peak, was better than 0.2 eV. The TEM samples were prepared by crushing powders of $SrCu_2(BO_3)_2$ crystal in high purity ethanol and depositing the solution on a holey carbon film. A detailed description of the growth, the structural and the magnetic properties of the $SrCu_2(BO_3)_2$ crystal used in these experiments, can be found

in Ref. 22. Neglecting the energy dependence of the dipole matrix element, the fine structure observed near the *O-K* edge can be simply interpreted as an image of the unoccupied O *p* projected density of states. As these states spread over a large energy range and experience a strong hybridization with orbitals of other atoms, they provide a good overall picture of the unoccupied states of transition-metal oxides. The theoretical spectrum calculated in LDA is shown in Fig. 3(a). This spectrum has been calculated in the dipole approximation using the TELNES.2 module of the WIEN2K code. The contributions arising from the two crystallographically inequivalent $O(1)$ and $O(2)$ sites have been taken into account with a relative weight of 1:2. Due to the strong anisotropy of the $SrCu_2(BO_3)_2$ crystal structure, the orientation dependence of the near-edge fine struture has been accounted for through a careful modeling of the experimental conditions used to record the spectra.[23] Finally, the energy spread of the electron source has been modeled through a Gaussian broadening of $\Gamma_{FWHM}=0.2$ eV and the finite lifetime effects modeled using an energy-dependent Lorentzian broadening of $\Gamma_{FWHM}=0.3+0.1(E-E_c)$, where E_c denotes the threshold energy. The constant part accounts for the finite lifetime of the O 1*s* core hole, whereas the energy-dependent part models the effect of the photoelectron finite lifetime following the empirical relation originally proposed by Weijs *et al.*[24] and justified later.[25] LDA provides a good description of high-lying structures (B)–(E) corresponding to the electronic states located in the continuum of the conduction band. Inspection of the different projected densities of states (not shown here) clarifies the origin of these structures. The first prominent peak (B) and the broad structures (D) and (E), separated by about 10 eV, are, respectively, related to unoccupied states of π^* and σ^* characters arising from antibonding combination of B 2*sp* and O 2*p* orbitals.[26,27] Between these strong signatures of the covalent B-O bond, peak (C) is associated with the Sr 4*d* bands. The main discrepancy between theoretical and experimental spectra comes from first peak (A), reflecting the O 2*p* component of the Cu-O $dp\sigma^*$ bands. The O 2*p* contribution is clearly overestimated and the energy position of these states with respect to the conduction band does not agree with the experiment. In addition, the metallic ground state obtained in LDA [Fig. 4(a)] is in clear contradiction with the insulating character found by resistivity measurements.[29] Spin-polarized solutions for both ferromagnetic and antiferromagnetic orders were found, the latter one being the most stable [see Fig. 5(a) for the exact spin arrangement].

The resulting electronic structure is shown in Fig. 4(b) and the corresponding theoretical *O-K* edge in Fig. 3(b). The exchange splitting affects essentially the Cu $d_{x^2-y^2}$ bands but is not sufficient to open a band gap. The resulting *O-K* edge is, however, in better agreement with the experimental results. This is merely due to the fact that, unlike Cu *d* states, the continuum of the conduction band is not spin polarized. It leads to a reduction of the intensity of peak (A) by a factor of 2 with respect to the other structures. The last important discrepancy is now the energy position of this peak with respect to the continuum, which is also intimately related to the presence of an energy gap between occupied and unoccupied states and thus to the insulating state of this compound. As already mentioned, the treatment of strongly correlated systems such as 3*d* transition-metal oxides requires to go beyond the mean field approach provided by LSDA. A series of calculations were performed using the "atomic limit" version of LDA+*U* proposed by Anisimov *et al.*[28] by varying the $U_{\text{eff}}=U-J^H$ parameter[30] from 0 to about 8 eV. The main effect of the LDA+*U* approach on the electronic structure of $SrCu_2(BO_3)_2$ is the splitting of the Cu $d_{x^2-y^2}$ states into a lower Hubbard band and an upper Hubbard band

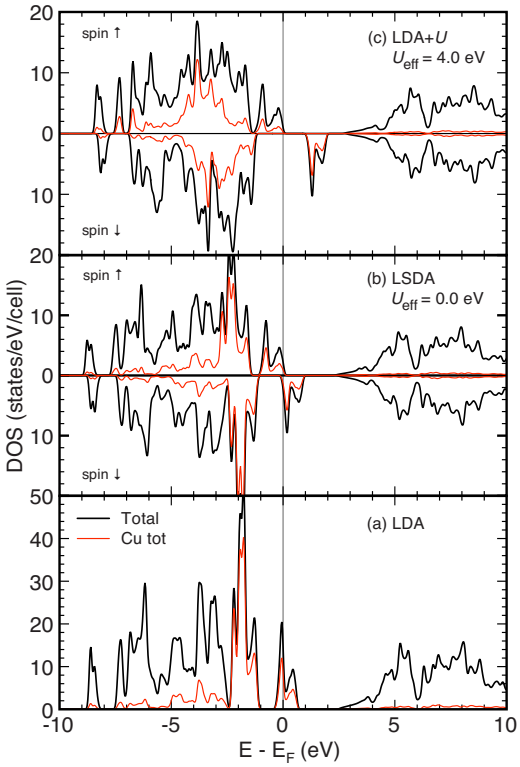

FIG. 4. (Color online) Electronic structure of $SrCu_2(BO_3)_2$ calculated for different approximations: (a) LDA, (b) LSDA ($U_{\text{eff}}=0.0$ eV), and (c) LDA+*U* as proposed by Anisimov *et al.* (Ref. 28) using $U_{\text{eff}}=U-J^H=4.0$ eV.

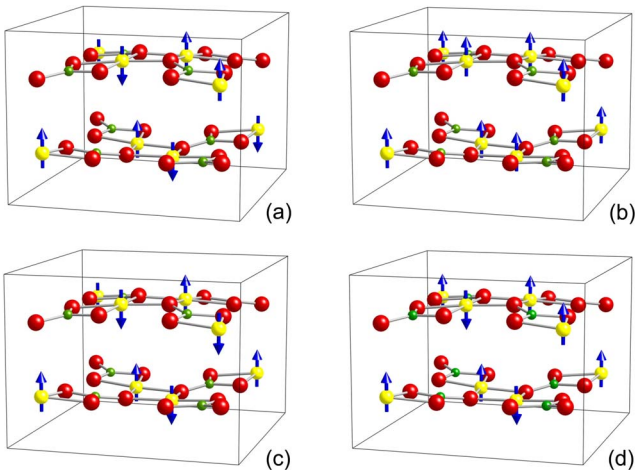

FIG. 5. (Color online) Four different spin arrangements used to calculate the exchange integrals *J*, *J′*, and *J″*. The Sr atoms are omitted for clarity.

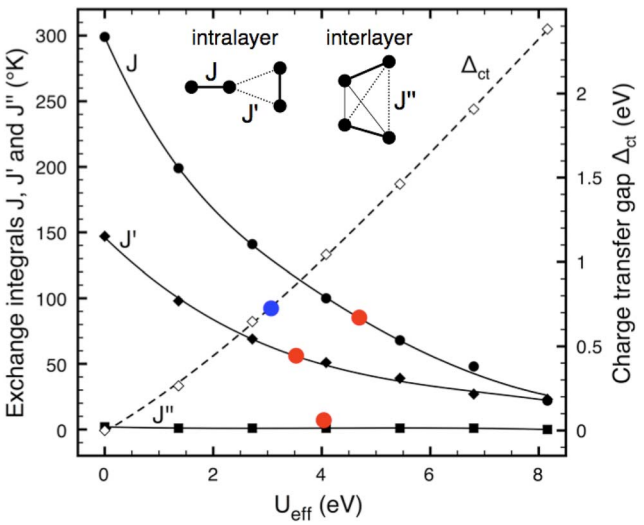

FIG. 6. (Color online) Evolution of the exchange integrals J, J', and J'' and the charge transfer gap Δ_{ct} in $SrCu_2(BO_3)_2$ as a function of U_{eff}. The experimental optical gap estimated from reflectance measurements (Ref. 32) is indicated in blue ($\Delta_{ct} \sim 0.70$ eV) and the experimental exchange integrals (Ref. 1) are represented by the red dots ($J=85$ K, $J'=54$ K, and $J''=8$ K).

(UHB), the position of which is fixed by the value of the U_{eff} parameter. This value has been determined so as to reproduce the energy position of the center of the UHB with respect to the conduction band found in the experimental *O-K* edge. A good agreement was found for U_{eff} in the range of 4.0–5.0 eV [Fig. 3(c)]. The resulting electronic structure [Fig. 4(c)] exhibits drastic changes with respect to LSDA. A correlation gap of ~1.00–1.35 eV depending on the exact value of U_{eff} now separates the UHB, primarily built from the Cu $d_{x^2-y^2}$ states, from the top of the valence band. The Cu $3d$ states participating to the valence band are now shifted down in energy with respect to LSDA thus resulting in a predominant O $2p$ character at the top of this band. The gap is therefore of charge transfer type, as expected for a late transition-metal oxide according to the theory of Zaanen *et al.*[31] It can be seen in the spectrum of Fig. 3(c) that this enhanced ionic character of the UHB further decreases the intensity of peak (A). This peak is also shifted toward higher energies and is now in better agreement with the experimental spectrum.

III. PROPERTIES

In order to assess the accuracy of LDA+U calculations in $SrCu_2(BO_3)_2$, it is first interesting to compare the calculated charge transfer gap with the optical gap measured experimentally. The variation of the charge transfer gap Δ_{ct} with the U_{eff} employed in the calculations is displayed in Fig. 6. To the best of our knowledge, a precise experimental value of the optical gap is not available in the literature. However, estimations from reflectance measurements[32] have been made and lead to a value of ~0.70 eV. This value corresponds to the charge transfer gap calculated with a U_{eff} slightly smaller than the range determined from the EELS experiments.

In a second part of this work, the exchange integrals between nearest neighbors J, next-nearest neighbors J' and between Cu atoms of adjacent layers J'' were determined as a function of U_{eff}. Strictly speaking, due to the slight buckling of the $[CuBO_3]^-$ layers, the Cu-Cu distance between dimers of adjacent planes is not constant. Therefore, two different interlayer couplings J''_1 and J''_2 should be defined. However, these exchange integrals are expected to be small and very similar, and we will only consider their average value J'' for simplicity. The supercell calculations required to compute these quantities were performed in the 44-atom tetragonal crystallographic cell for four different collinear spin arrangements of the Cu^{2+} atoms displayed in Fig. 5. Configuration (a) corresponds to an antiferromagnetic (AFM) arrangement of the spins inside each dimer and is the most stable solution for all values of U_{eff}. Configuration (b) is the usual ferromagnetic (FM) order. Configurations (c) and (d) correspond to slightly more complicated arrangements. In (c), adjacent dimers inside the same layer have different (FM or AFM) arrangements in such a way that each AFM (respectively, FM) dimer is surrounded by four FM (respectively, AFM) dimers. In addition, an AFM arrangement is introduced along the [001] columns of FM dimers. Configuration (d) shares the same arrangement as (c) within the layers, but the FM dimers have a FM arrangement along the [001] columns. Using the Ising solutions of Hamiltonian (1), one obtains the set of equations,

$$E_{(a)} = E_0 - 4J,$$

$$E_{(b)} = E_0 + 4J + 16J' + 16J'',$$

$$E_{(c)} = E_0 - 8J'',$$

$$E_{(d)} = E_0 + 8J''.$$

Therefore, after calculating the total energies of the tetragonal cell for the four different spin arrangements, the exchange integrals are simply obtained by inverting the previous set of equations,

$$J = (E_{(c)} + E_{(d)} - 2E_{(a)})/8,$$

$$J' = (E_{(a)} + E_{(b)} - 2E_{(d)})/16,$$

$$J'' = (E_{(d)} - E_{(c)})/16.$$

Their evolution with U_{eff} is displayed in Fig. 6. It should be noted that this approach neglects the effects of quantum fluctuations. As a consequence, these calculations may overestimate[30] the actual values of J and J' by about 15%–20%. Besides the negligible value found for J'' (~1 K), J and J' exhibit the same monotonic decrease as U_{eff} increases, consistent with the asymptotic behavior $4t^2/U_{\text{eff}}$ expected in the strongly correlated limit. The values of J and J' calculated in LSDA ($U_{\text{eff}}=0.0$ eV) are more than three times larger than the experimental values. However, Fig. 6 clearly indicates that both J and J' reach their experimental values for a U_{eff} around 4–5 eV, in total agreement with the value estimated from the EELS results. Whereas superexchange

paths are well defined through the covalent Cu-O-Cu and Cu-O-B-O-Cu bonds for J and J', the interplane interaction can only take place through the Sr^{2+} ions. The absence of Sr states in the electronic structure of $SrCu_2(BO_3)_2$ between the semicore $4p$ states and the high-lying $4d$ and $5s$ states explains the negligible value found for J''.

IV. CONCLUSION

From this comparison between experiments and theory, we have been able to show that a careful modeling of the *O-K* near-edge fine structure leads to a reasonable estimation of the effective Hubbard term to be employed in the calculation of the electronic structure of $SrCu_2(BO_3)_2$ with the LDA+U method. The determination of this parameter is a crucial starting point to access other related properties using first-principles calculations. In $SrCu_2(BO_3)_2$, we demonstrated that the LDA+U method not only provides a good description of the insulating state of this compound but allows an accurate determination of the exchange integrals J and J' governing its magnetic properties. Furthermore, EELS is one of the rare solid-state spectroscopies with which the atomic-column spatial resolution can be achieved. The methodology reported here, and in particular, the use of the *O-K* near-edge fine structure as a guide to model the electronic structure of complex copper oxides, is thus promising in studies where such a high-spatial resolution is required.

ACKNOWLEDGMENTS

We would like to thank R. Hayn for helpful discussions and comments on this work and S. Dordevic and C. Homes for communicating to us the value of the optical gap of $SrCu_2(BO_3)_2$. We also thank S. Lazar (now with FEI Company, Eindhoven, The Netherlands) for his help in the acquisition of the EELS results.

*guillaume.radtke@univ-cezanne.fr

[1] S. Miyahara and K. Ueda, J. Phys.: Condens. Matter **15**, R327 (2003).
[2] H. Kageyama, K. Yoshimura, R. Stern, N. V. Mushnikov, K. Onizuka, M. Kato, K. Kosuge, C. P. Slichter, T. Goto, and Y. Ueda, Phys. Rev. Lett. **82**, 3168 (1999).
[3] H. Kageyama, K. Onizuka, T. Yamauchi, Y. Ueda, S. Hane, H. Mitamura, T. Goto, K. Yoshimura, and K. Kosuge, J. Phys. Soc. Jpn. **68**, 1821 (1999).
[4] H. Kageyama, M. Nishi, N. Aso, K. Onizuka, T. Yosihama, K. Nukui, K. Kodama, K. Kakurai, and Y. Ueda, Phys. Rev. Lett. **84**, 5876 (2000).
[5] K. Kodama, M. Takigawa, M. Horvatic, C. Berthier, H. Kageyama, Y. Ueda, S. Miyahara, F. Becca, and F. Mila, Science **298**, 395 (2002).
[6] G. A. Jorge, R. Stern, M. Jaime, N. Harrison, J. Bonča, S. El Shawish, C. D. Batista, H. A. Dabkowska, and B. D. Gaulin, Phys. Rev. B **71**, 092403 (2005).
[7] S. Miyahara and K. Ueda, Phys. Rev. Lett. **82**, 3701 (1999).
[8] S. Miyahara and K. Ueda, Phys. Rev. B **61**, 3417 (2000).
[9] Zheng Weihong, C. J. Hamer, and J. Oitmaa, Phys. Rev. B **60**, 6608 (1999).
[10] A. Koga and N. Kawakami, Phys. Rev. Lett. **84**, 4461 (2000).
[11] C.-H. Chung and Y. B. Kim, Phys. Rev. Lett. **93**, 207004 (2004).
[12] R. W. Smith and D. A. Kesler, J. Solid State Chem. **93**, 430 (1991).
[13] B. S. Shastry and B. Sutherland, Physica B & C **108B**, 1069 (1981).
[14] S. Miyahara and K. Ueda, J. Phys. Soc. Jpn. **69**, 72 (2000).
[15] M. T. Czyżyk and G. A. Sawatzky, Phys. Rev. B **49**, 14211 (1994).
[16] P. Blaha, K. Schwarz, G. Madsen, D. Kvaniscka, and J. Luitz, in *Wien2k, An Augmented Plane Wave+Local Orbitals Program for Calculating Crystal Properties*, edited by K. Schwarz (Technische Universitat Wien, Austria, 2001).
[17] S. L. Dudarev, G. A. Botton, S. Y. Savrasov, C. J. Humphreys, and A. P. Sutton, Phys. Rev. B **57**, 1505 (1998).
[18] S. Dudarev, M. Castell, G. Botton, S. Savrasov, C. Muggelberg, G. Briggs, A. Sutton, and D. Goddard, Micron **31**, 363 (2000).
[19] L. V. Dobysheva, P. L. Potapov, and D. Schryvers, Phys. Rev. B **69**, 184404 (2004).
[20] J. P. Perdew and Y. Wang, Phys. Rev. B **45**, 13244 (1992).
[21] S. Lazar, G. Botton, M.-Y. Wu, F. Tichelaar, and H. Zandbergen, Ultramicroscopy **96**, 535 (2003).
[22] H. Dabkowska, A. Dabkowski, G. Luke, S. Dunsiger, S. Haravifard, M. Cecchinel, and B. Gaulin, J. Cryst. Growth **306**, 123 (2007).
[23] C. Hébert, P. Schattschneider, H. Franco, and B. Jouffrey, Ultramicroscopy **106**, 1139 (2006).
[24] P. J. W. Weijs, M. T. Czyżyk, J. F. van Acker, W. Speier, J. B. Goedkoop, H. van Leuken, H. J. M. Hendrix, R. A. de Groot, G. van der Laan, K. H. J. Buschow, G. Wiech, and J. C. Fuggle, Phys. Rev. B **41**, 11899 (1990).
[25] C. Hébert, M. Kostner, and P. Schattschneider, Conference Proceeding of EUREM XII (Brno), 2000, p. 333.
[26] D. Vaughan and J. Tossel, Am. Mineral. **58**, 765 (1973).
[27] L. A. J. Garvie, A. J. Craven, and R. Brydson, Am. Mineral. **80**, 1132 (1995).
[28] V. I. Anisimov, I. V. Solovyev, M. A. Korotin, M. T. Czyżyk, and G. A. Sawatzky, Phys. Rev. B **48**, 16929 (1993).
[29] G. T. Liu, J. L. Luo, N. L. Wang, X. N. Jing, D. Jin, T. Xiang, and Z. H. Wu, Phys. Rev. B **71**, 014441 (2005).
[30] A. N. Yaresko, A. Y. Perlov, R. Hayn, and H. Rosner, Phys. Rev. B **65**, 115111 (2002).
[31] J. Zaanen, G. A. Sawatzky, and J. W. Allen, Phys. Rev. Lett. **55**, 418 (1985).
[32] S. Dordevic and C. Homes (private communication).